



Measurement of the Top Quark Mass in the Electron-Muon Channel using the Matrix Element Method with 3.6 fb^{-1}

Results for Winter 2009 Conferences
The DØ Collaboration
(Dated: March 13, 2009)

A measurement of the top quark mass in the electron-muon channel using the matrix element method is presented. This measurement is performed on a data sample of about 3.6 fb^{-1} collected by the DØ experiment in Run II of the Fermilab Tevatron collider at a center-of-mass energy of $\sqrt{s}=1.96 \text{ TeV}$. We apply kinematic cuts to select events that are consistent with $t\bar{t}$ decaying into one electron, one muon, two b quarks, and neutrinos. We select 154 data events in which we expect 118 $t\bar{t}$ events. We form a likelihood function as the convolution of the leading order matrix element and detector resolution functions for each of these 115 events as a function of the top quark mass and extract from the product of them the measured top quark mass:

$$\begin{aligned}m_{\text{top}}^{e\mu}(\text{Run IIa}) &= 171.7 \pm 6.4 (\text{stat.}) \pm 2.5(\text{syst.}) \text{ GeV} \\m_{\text{top}}^{e\mu}(\text{Run IIb}) &= 176.1 \pm 3.9 (\text{stat.}) \pm 2.7(\text{syst.}) \text{ GeV} \\m_{\text{top}}^{e\mu}(\text{comb.}) &= 174.8 \pm 3.3 (\text{stat.}) \pm 2.6 (\text{syst.}) \text{ GeV}\end{aligned}$$

for the Run IIa, Run IIb, and the combined data set. Combining these results with the Run IIa ones using the neutrino weighting method and the matrix weighting method in the dielectron, dimuon and lepton+isolated track channels leads to the following measured top mass:

$$m_{\text{top}}^{\ell\ell}(\text{comb.}) = 174.7 \pm 2.9 (\text{stat.}) \pm 2.4 (\text{syst.}) \text{ GeV}$$

I. INTRODUCTION

The top quark was discovered in 1995 by the CDF and DØ experiments at the Fermilab Tevatron proton anti-proton collider [1, 2]. A precise measurement of the top mass m_{top} constrains the mass of the yet unobserved Higgs boson through radiative corrections to the W mass and can restrict possible extensions to the standard model (SM) [3].

The Tevatron is still the only place where top quarks can be produced and studied directly. At the Tevatron, top quarks are mostly produced in pairs via the strong interaction. A (anti-) top quark is predicted to decay almost exclusively to a W boson and an (anti-) b quark. Events from top quark pair production are classified according to the decay channels of the W bosons. An event is referred to as dilepton if both W bosons decay leptonically. This channel has a small branching ratio compared to the one in which exactly one W boson decays hadronically (the ℓ +jets channel) but also contains less background. Among the dilepton channels, the one where one W boson decays into an electron and the other into a muon and corresponding neutrinos has the largest branching ratio and fewer background (especially from Z +jets events). A systematic difference between top quark masses measured from different decay channels could indicate contributions from new processes beyond the SM.

The reconstruction of the top mass from dilepton events poses a particular challenge as the two neutrinos from the W boson decays are undetected. To extract the maximum information from the limited dilepton event sample, we use the matrix element method. This method was pioneered and first applied to measure the top quark mass in the ℓ +jets channel [4] and then applied to dilepton events in [5]. We present here the first measurement in the dilepton channel by the DØ collaboration combining the separate Run IIa (April 2002 to February 2006) and Run IIb (June 2006 to December 2008) data sets.

II. EVENT SELECTION

This analysis is based on an integrated luminosity of 3.6 fb^{-1} collected with the DØ detector from April 2002 to December 2008. The event selection is designed to define a data sample enriched in top quark pair events. An event is required to contain an isolated electron with $p_{\text{T}} > 15 \text{ GeV}$ and a pseudorapidity $|\eta| < 1.1$ or $1.5 < |\eta| < 2.5$ and an isolated muon with $p_{\text{T}} > 15 \text{ GeV}$ and $|\eta| < 2$. The event vertex must be within 60 cm of the center of the detector along the beam direction. The event is also required to have at least two jets with $p_{\text{T}} > 20 \text{ GeV}$ and $|\eta| < 2.5$. For Run IIa, we require in addition the leading jet to have a $p_{\text{T}} > 30 \text{ GeV}$. Finally, the topological variable H_{T} defined as the scalar sum of the transverse momenta of the leading lepton and the two leading jets is required to be greater than 115 GeV for Run IIa and greater than 105 GeV for Run IIb.

Background contribution to the electron-muon channel come first from the Z boson production with associated jets where the Z boson decays into two tau leptons that further decay leptonically ($Z \rightarrow \tau\tau \rightarrow e\mu$ +jets). Other background processes come from diboson production (WW , WZ +jets), and from events in which a jet is misidentified as an electron, and the production of heavy hadrons which decay into leptons which pass the isolation requirements. (The latter two are referred to as “fake” lepton backgrounds.) The Z boson and diboson backgrounds are evaluated using Monte Carlo (MC), and the fake background is measured using data. Table I shows the predicted and observed numbers of events after the selection for both the Run IIa and Run IIb data periods.

	$t\bar{t} \rightarrow e\mu$	$Z \rightarrow \tau\tau \rightarrow e\mu$	WW, WZ	fake e	fake isolated μ	total	observed
Run IIa	$36.8^{+2.6}_{-2.7}$	$6.0^{+0.9}_{-1.0}$	$1.6^{+0.4}_{-0.4}$	$0.8^{+0.3}_{-0.2}$	$1.9^{+0.5}_{-0.5}$	$46.9^{+3.4}_{-3.6}$	39
Run IIb	$81.7^{+0.3}_{-0.3}$	$3.8^{+0.8}_{-0.8}$	$4.4^{+0.4}_{-0.4}$	$2.6^{+0.7}_{-0.6}$	$2.1^{+0.9}_{-0.8}$	$94.5^{+1.4}_{-1.4}$	115

TABLE I: Final number of expected and observed events and their statistical and systematic uncertainties in the $e\mu$ channel after all cuts for Run IIa (upper row) and Run IIb (lower row).

III. THE MATRIX ELEMENT METHOD

The analysis method is designed to fully exploit the kinematic information in the data sample. We compute the probabilities for each event to arise from background or signal of some assumed top quark mass m_{top} . These probabilities are then combined over the entire data sample to produce a likelihood as a function of m_{top} . The measurement is then extracted by maximizing the likelihood with respect to the top quark mass.

The probability P_{evt} for each event is composed from the probabilities for two processes, top quark pair production and $Z \rightarrow \tau\tau$ + jets production as:

$$P_{\text{evt}}(x, m_{\text{top}}) = f_{\text{top}} \cdot P_{\text{sgn}}(x; m_{\text{top}}) + (1 - f_{\text{top}}) \cdot P_{\text{bkg}}(x). \quad (1)$$

Here, x denotes the object four-vectors of the event, f_{top} the signal fraction in the sample given (fixed by the number of expected events in Table I), P_{sgn} and P_{bkg} the probability densities for observing x given a top quark pair and a $Z \rightarrow \tau\tau + \text{jets}$ production event, respectively. For simplicity, only the $Z \rightarrow \tau\tau + \text{jets}$ matrix element is used to compute P_{bkg} . It has been shown that the omission of the other backgrounds does not cause a significant bias. To evaluate the probabilities, we integrate over quantities that are unknown because they are unmeasured by the detector such as neutrino energies.

The differential probability to observe a top quark event with final-state x in the detector is given by:

$$P_{\text{sgn}}(x; m_{\text{top}}) = \frac{1}{\sigma_{\text{obs}}(q\bar{q} \rightarrow t\bar{t} \rightarrow e\mu; m_{\text{top}})} \cdot \int_{q_1, q_2, y} \sum_{\text{flavors}} dq_1 dq_2 f(q_1) f(q_2) \frac{(2\pi)^4 |\mathcal{M}|^2}{4\sqrt{(q_1 \cdot q_2)^2}} \cdot d\Phi_6 \cdot W(x, y). \quad (2)$$

Here, \mathcal{M} denotes the matrix element for the process $q\bar{q} \rightarrow t\bar{t} \rightarrow e\mu\nu_e\nu_\mu b\bar{b}$, q_1 and q_2 the momentum fractions of the colliding quarks within the proton and anti-proton, $d\Phi_6$ an element of six-body phase space, and the parton density function (PDF) $f(q)$ the probability to find a quark of given flavor and momentum fraction q in the proton or anti-proton. The finite detector resolution is taken into account via the convolution with a transfer function $W(x, y)$ that describes the probability to reconstruct a partonic final state y as x in the detector. The angles of all measured decay products are assumed to be well-measured. The jet and muon transverse momentum resolutions are determined from data. Since it is not known from which parton the two leading jets originate, a sum over the two possible permutations of jet-to-parton assignments is performed.

The overall detector efficiency depends on m_{top} . This is taken into account in the normalization of P_{sgn} which is computed as:

$$\sigma_{\text{obs}}(m_{\text{top}}) = \int_{x, y} d^n \sigma(y; m_{\text{top}}) W(x, y) \Theta_{\text{acc}}(x) dx, \quad (3)$$

where $\Theta_{\text{acc}}(x)$ is 1 if an event passes our selection criteria, and 0 otherwise.

As the integration in (2) is also performed over the unknown transverse momentum of the $t\bar{t}$ pair, the matrix element for each event is also multiplied by the probability for such an event to have the assumed $p_T(t\bar{t})$. This probability is evaluated using ALPGEN [7] MC events both for events with exactly two reconstructed jets and events with more than two jets.

The expression for the background probability P_{bkg} is similar to that for P_{sgn} except that the VECBOS [8] parametrization of the matrix element \mathcal{M} is used. An additional transfer function is then used to relate the energies of the tau leptons to those of their electron or muon decay products. Since the matrix element for $Z \rightarrow \tau\tau + \text{jets}$ production does not depend on m_{top} , P_{bkg} is independent of m_{top} .

In order to extract the top quark mass from a set of n measured events x_1, \dots, x_n , a likelihood function is built from the event probabilities,

$$L(x_1, \dots, x_n; m_{\text{top}}) = \prod_{i=1}^n P_{\text{evt}}(x_i; m_{\text{top}}), \quad (4)$$

and evaluated for different hypotheses of m_{top} . The top quark mass is finally determined by minimizing

$$-\ln L(x_1, \dots, x_n; m_{\text{top}}) = -\sum_{i=1}^n \ln(P_{\text{evt}}(x_i; m_{\text{top}})) \quad (5)$$

with respect to m_{top} .

IV. CALIBRATION OF THE METHOD

Ensemble testing is used to correct for any bias in the extracted top quark mass as well as to ensure that the estimated uncertainty is reliable. Such biases occur when the assumptions used to derive the probabilities are violated, such as that the jet and lepton angles are perfectly measured. An ensemble of pseudo-experiments is formed by randomly

drawing top quark signal events and $Z \rightarrow \tau\tau + \text{jets}$ or WW events from a large pool of simulated MC events. Fake events are also introduced in the pseudo-experiments using data events where the electron and the muon has the same charge and where the muon is loosely isolated. The total size of each pseudo-experiment is fixed to the number of events in data while the relative proportions of signal and background are allowed to fluctuate around the values from Table I. This procedure is repeated 1000 times. The fitted top quark masses and the widths of the pull distributions from each pseudo-experiment are plotted as a function of the true top quark mass. These are then fitted to straight lines, which are used later to calibrate the data results. Figure 1 shows the final calibration curve for Run IIa, Figure 2 the one for Run IIb.

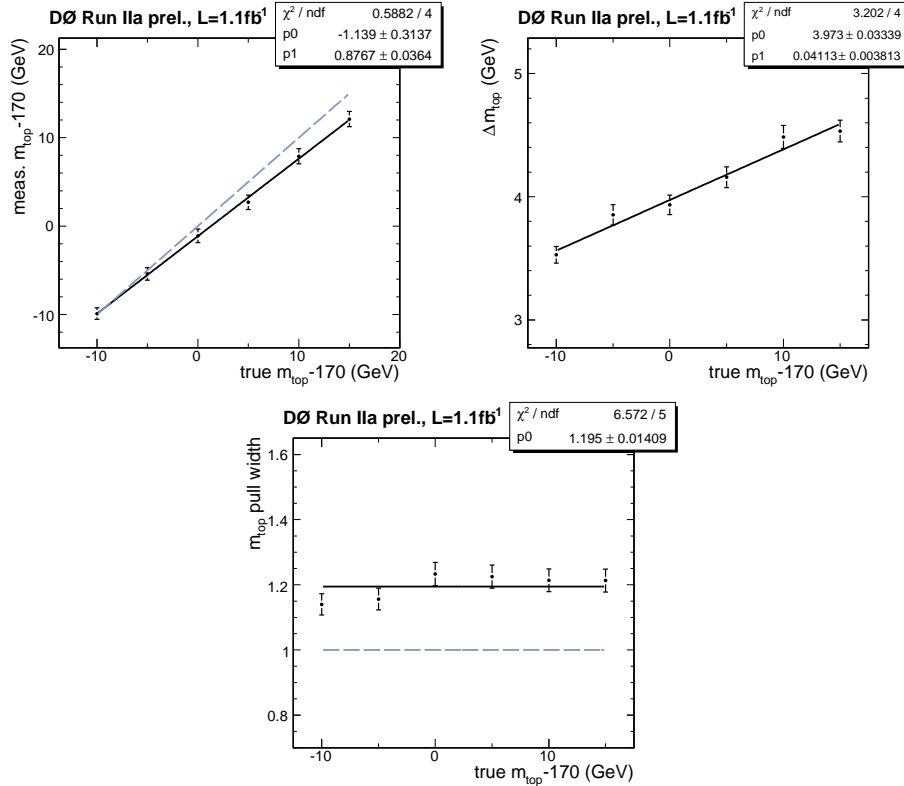


FIG. 1: m_{top} calibration curve, the statistical uncertainty and pull width are shown using signal and background events in the $e\mu$ channel requiring at least two jets for Run IIa. The solid lines show the fit to the points while the dashed ones show the perfect cases with no bias.

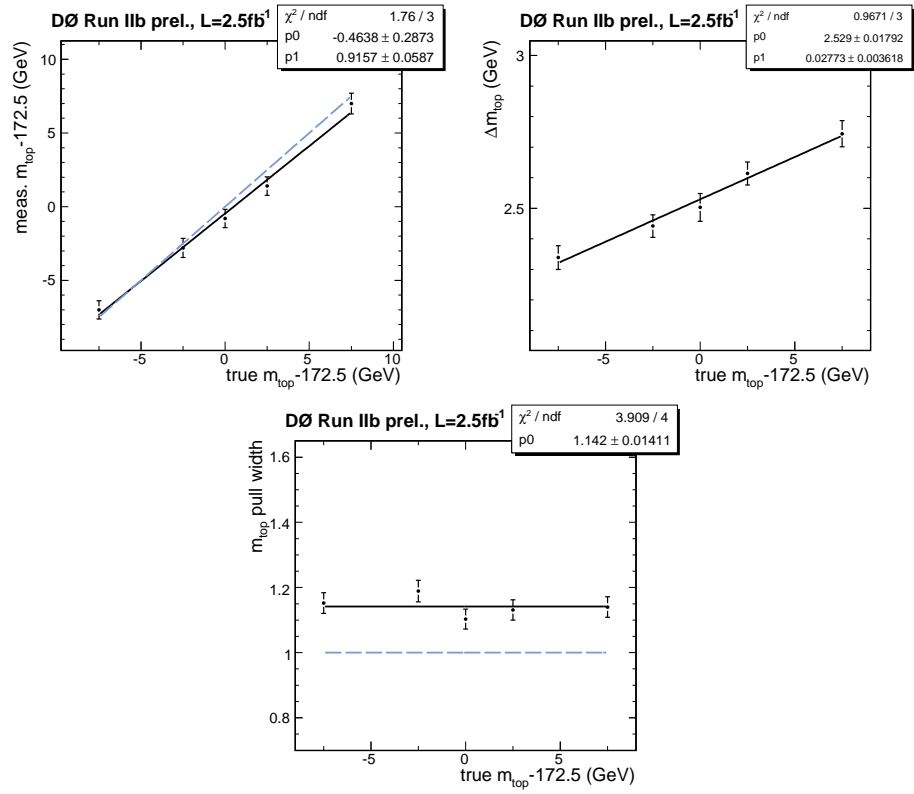


FIG. 2: m_{top} calibration curve, the statistical uncertainty and pull width are shown using signal and background events in the $e\mu$ channel requiring at least two jets for Run IIb. The solid lines show the fit to the points while the dashed ones show the perfect cases with no bias.

V. SYSTEMATIC UNCERTAINTIES

- **Jet Energy Scale (JES) systematics.** This systematic uncertainty has been evaluated by shifting the jet energy scale corrections by -1σ or $+1\sigma$ where σ is the JES uncertainty measured from γ +jets and dijet events.
- **b/light jet response.** This uncertainty takes into account the difference between the nominal inclusive response and the response for b hadrons. The *b/light* response ratio between data and simulation has been evaluated to be 1.8 %. This uncertainty is then obtained by shifting the nominal response down by 1.8 % and deriving a new calibration curve.
- **Jet resolution systematics.** The resolution of jets in simulated data is better than that of jets in real data. Therefore, simulated jets have extra smearing applied in order to match the data. To evaluate the effect of the uncertainty in the jet energy resolution, an ensemble test is done with MC samples in which the extra jet smearing has been increased or decreased by $\pm 1\sigma$, where σ is the jet energy resolution uncertainty.
- **Sample-dependent JES.** The jet energy scale corrections in MC are shifted to take into account the difference with respect to data. The shifting is different for quark jets and for gluon jets. A systematic uncertainty is introduced to take into account this sample-dependent jet energy scale. It is given by the change in the extracted top mass from MC when the jet energy scale shifting is turned on or off in $t\bar{t}$ MC samples.
- **Muon resolution systematics.** Similarly to jets, muon momenta require extra smearing in order to match the data. The uncertainty due to this is evaluated in the same manner as that due to the jet resolution uncertainty. An ensemble test is done with MC samples in which the extra muon smearing has been shifted by -1σ down or $+1\sigma$ up where σ is the muon momentum resolution uncertainty.
- **b quark modeling uncertainty.** Possible effects are studied by reweighting the simulated top quark pair events used in the calibration to simulate the choice of different fragmentation models for the b jets. The samples have been reweighted either to a Bowler scheme [10] that has been tuned to LEP data or to a model tuned to SLD data [11]. The largest difference with respect to the nominal measured top mass is taken as the b quark fragmentation systematic uncertainty.
- **PDF uncertainties.** The systematic uncertainty due to the choice of PDF is estimated by varying the 20 CTEQ6.1M PDF eigenvalues within their uncertainties in the $t\bar{t}$ signal MC. Variations for each parameter have been used as an additional event weight which is taken into account by the ensemble testing procedure. The resulting PDF uncertainty is a quadratic sum of those due to the 20 individual parameters.
- **MC calibration.** This uncertainty is estimated by varying the calibration of the top quark mass measurement according to the statistical uncertainty of the linear fit of the calibration curve.
- **Signal fraction.** This uncertainty reflects the uncertainty on the number of expected background events. To estimate the uncertainty, the number of background events was scaled up and down by 1σ while the number of signal events was scaled down and up by 1σ , while building ensembles. The calibration curve with these modified ensembles has been rederived to estimate the systematic uncertainty.
- **QCD background modeling.** This uncertainty reflects the uncertainty on the shape of the fake background that is used for the calibration. The muon loose isolation criteria has been varied in the same sign events used in the ensemble testing. The resulting difference on the measured mass is quoted as systematic uncertainty.
- **Lepton momentum scale.** This uncertainty reflects the difference between data and MC on the absolute lepton momentum measurement.
- **Hadronization and underlying event** The systematic uncertainty coming from different hadronization and underlying event model is taken from the difference between the result using Pythia and Herwig.
- **Initial state radiation (ISR) and final state radiation (FSR)** This systematic uncertainty is evaluated comparing the result using PYTHIA with ISR and FSR parameters varied up and down. These parameters were tuned to Drell-Yan data by the CDF collaboration [12].
- **Color Reconnection** Various Pythia tunes using different models of color reconnection are investigated. These effects on the top mass measurement from a MC-truth level study are found to be about 0.5GeV [13]. After preliminary estimation, the comparison between Pythia tuneApro and Pythia tuneACRpro performed with the full simulation agrees with the MC-truth level study. For this preliminary result, we assign a 0.4 GeV uncertainty for the color reconnection effects.

Uncertainty	$e\mu$ Run IIa [GeV]	$e\mu$ Run IIb [GeV]
JES	+1.2 -1.3	+1.5 -1.6
b/light quark response	± 1.4	± 1.6
jet resolution	+0.6 -0.6	+0.2 -0.3
sample-dependent JES	± 0.2	± 0.1
muon smearing	+0.3 -0.0	± 0.3
b quark modeling	± 0.1	± 0.3
PDF uncertainty	+0.3 -0.0	+0.1 -0.2
MC calibration	± 0.4	± 0.4
signal fraction	+0.2 -0.0	± 0.3
QCD background modeling	± 0.6	± 0.6
electron energy scale	± 0.1	± 0.1
muon momentum scale	± 0.2	± 0.2
hadronization and UE	± 1.0	± 1.0
ISR/FSR	± 0.6	± 0.6
Color reconnection	± 0.4	± 0.4
TOTAL	± 2.4	± 2.6

TABLE II: Summary of systematic uncertainties.

Table II summarizes all systematic uncertainties on the top quark mass measurement with the matrix element method. The total systematic uncertainty on the top quark mass measurement is obtained by adding all contributions in quadrature:

$$(\Delta m_{\text{top}})_{\text{syst}}^{e\mu \text{ Run IIa}} = \pm 2.4 \text{ GeV}, \quad (6)$$

$$(\Delta m_{\text{top}})_{\text{syst}}^{e\mu \text{ Run IIb}} = \pm 2.6 \text{ GeV}. \quad (7)$$

VI. RESULT FROM DATA

The matrix element method is applied to the 3.6 fb^{-1} data set collected by $D\bar{O}$ during Runs IIa and IIb. The uncalibrated fit results are shown in Figure 3. These results are then corrected taking into account the calibration curves derived in Section IV (see Figure 1 and 2). Table III summarizes the uncalibrated and the calibrated results for the two jet inclusive selection. The corrected statistical uncertainty yielded by the likelihood fit is adjusted according to the deviation of the pull from unity; the fitted mass is also shifted accordingly. The top quark mass is measured to be

$$m_{\text{top}}^{e\mu \text{ Run IIa}} = 171.7 \pm 6.4 \text{ (stat.) GeV} \quad (8)$$

$$m_{\text{top}}^{e\mu \text{ Run IIb}} = 176.1 \pm 3.9 \text{ (stat.) GeV} \quad (9)$$

The distributions of calibrated statistical uncertainties from ensemble tests for $m_{\text{top}} = 170 \text{ GeV}$ for Run IIa and $m_{\text{top}} = 180 \text{ GeV}$ from Run IIb are shown in Figure 4. The combination of the two top quark mass results has been

channel	$m_{\text{top}}^{\text{unclb}}$ (GeV)	$m_{\text{top}}^{\text{clb}}$ (GeV)
$e\mu$ Run IIa	$170.4 \pm 4.7 \text{ (stat.)}$	$171.7 \pm 6.4 \text{ (stat.)}$
$e\mu$ Run IIb	$175.3 \pm 3.1 \text{ (stat.)}$	$176.1 \pm 3.9 \text{ (stat.)}$

TABLE III: Fitted top quark masses for the $e\mu$ channel in Runs IIa and IIb. The values in the left column are uncalibrated, the ones in the right are calibrated.

performed using the BLUE method [14]. We used the same uncertainty classes and method as used by the Tevatron Electroweak Working Group in their top mass combination [15]. All uncertainties are taken to be fully correlated between Run IIa and Run IIb except the statistical and the fit uncertainties. The result for the full Run II data set for the electron-muon channel is:

$$\begin{aligned} m_{\text{top}}^{e\mu} &= 174.8 \pm 3.3 \text{ (stat.)} \pm 2.6 \text{ (syst.) GeV or} \\ &= 174.8 \pm 4.2 \text{ GeV.} \end{aligned}$$

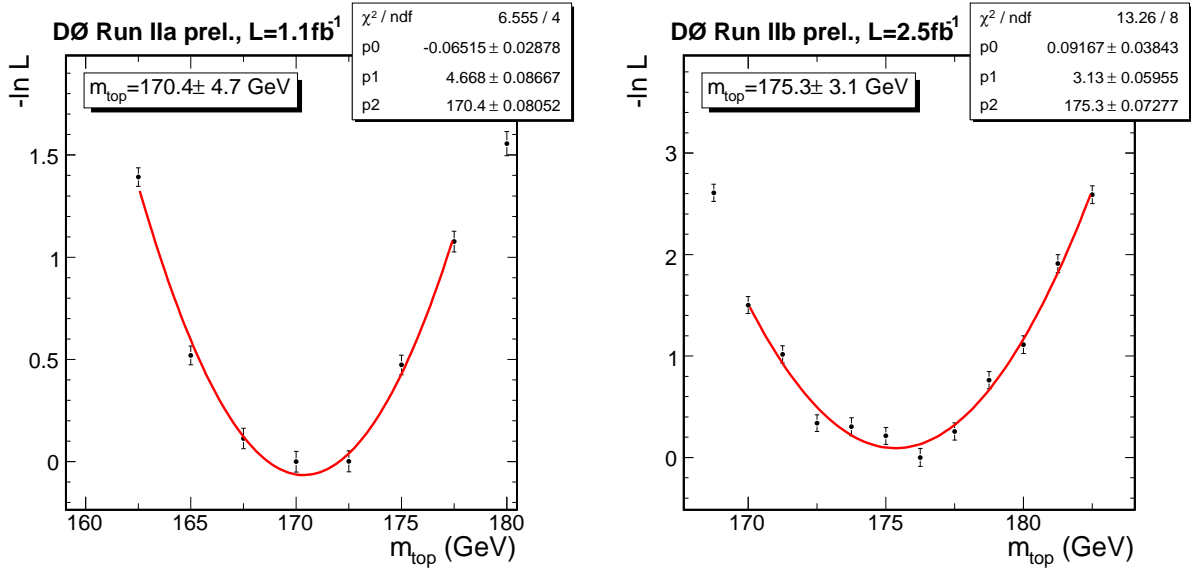


FIG. 3: Application of the matrix element method to the Run IIa and Run IIb data set in the $e\mu$ channel (uncalibrated). The left plot is for Run IIa data and the right one for Run IIb data.

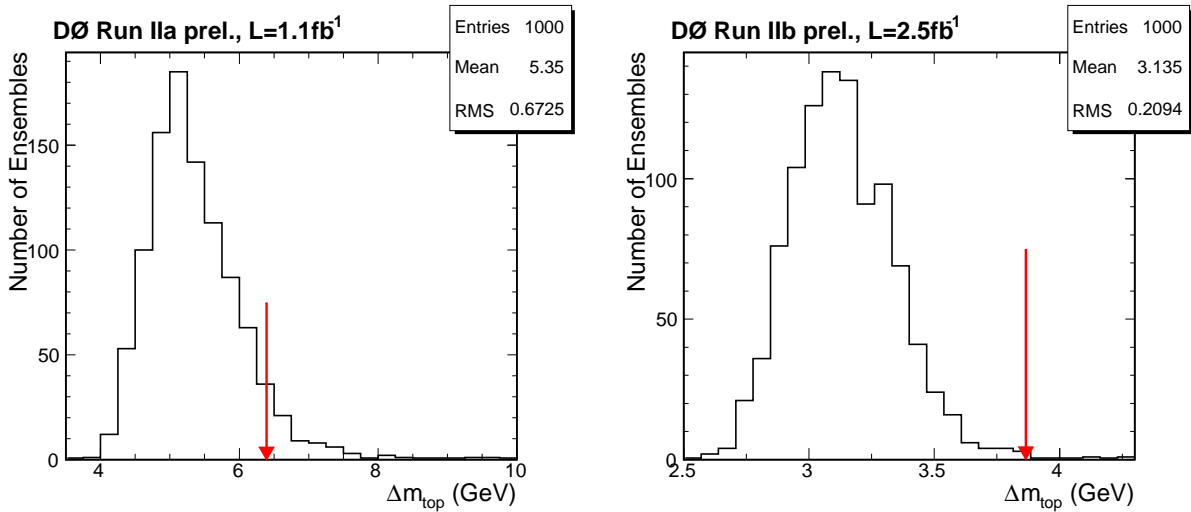


FIG. 4: Calibrated statistical uncertainty distributions for the $e\mu$ Run IIa (left) and Run IIb (right) measurement. The arrows indicate the measured statistical uncertainty in data.

The combination yields a χ^2 of 0.34 for 1 degree of freedom, which corresponds to a probability of 56%.

We can further combine this measurement with the measurements using two electrons and two muons (ee and $\mu\mu$ channels) and using one lepton and one isolated track ($\ell + track$ channel) performed using the neutrino weighting method and the matrix weighting method [16].

Table IV summarizes the top quark mass measurements that enter the combination with the corresponding statistical and systematic uncertainties. The uncertainties definition follows the one defined in [15].

All uncertainties defined in Table IV are taken to be fully correlated among the channels except for the statistical and the fit uncertainties that are uncorrelated between channels.

The result for the combination of these four channels is:

$$\begin{aligned}
 m_{\text{top}}^{\ell\ell} &= 174.7 \pm 2.9 \text{ (stat.)} \pm 2.4 \text{ (sys.) GeV or} \\
 &= 174.7 \pm 3.8 \text{ GeV.}
 \end{aligned}$$

	Run II		
	$e\mu$ Run IIa	$e\mu$ Run IIb	$ee + \mu\mu$ Run IIa + $\ell + track$ Run IIa
lumi	1.0 fb^{-1}	2.6 fb^{-1}	1 fb^{-1}
top quark mass	171.7 GeV	176.1 GeV	174.2 GeV
iJES	0.00	0.00	0.00
aJES	1.52	1.62	0.57
bJES	0.10	0.30	0.30
cJES	0.00	0.00	0.00
dJES	1.27	1.55	1.43
rJES	0.00	0.00	0.00
Leppt	0.27	0.37	0.26
Signal	0.62	0.62	0.75
MC	1.00	1.00	1.00
UN/MI	0.00	0.00	0.00
Background	0.00	0.00	0.30
Fit	0.73	0.78	1.00
CR	0.40	0.40	0.40
MHI	0.00	0.00	0.00
total systematic	2.50	2.74	2.4
statistical	6.40	3.90	6.0
total	6.87	4.77	6.46

TABLE IV: Inputs to the $D\bar{O}$ dilepton top quark mass combination. Uncertainties are in GeV. The uncertainties definition follows the one defined in [15].

The combination yields a χ^2 of 0.35 for 2 degrees of freedom, which corresponds to a probability of 84%.

-
- [1] CDF Collaboration, F. Abe et al., Phys. Rev. Lett. **74**, 2626 (1995).
[2] $D\bar{O}$ Collaboration, S. Abachi et al., Phys. Rev. Lett. **74**, 2632 (1995).
[3] S. Heinemeyer et al., *Physics Impact of a Precise Determination of the Top Quark Mass at an $e+e-$ Linear Collider*, JHEP 0309, 075 (2003).
[4] $D\bar{O}$ Collaboration, V.M. Abazov et al., Nature **429**, 638 (2004).
[5] CDF Collaboration, A. Abulencia et al., Phys. Rev. Lett. **96**, 152002 (2006).
[6] N. Kidonakis, *A unified approach to NNLO soft and virtual corrections in electroweak, Higgs, QCD and SUSY processes*, hep-ph/0303186
N. Kidonakis, private communication.
[7] M.L. Mangano et al., *ALPGEN, a Generator for Hard Multiparton Processes in Hadronic Collisions*, JHEP 307, 1 (2003).
[8] F.A. Berends, H. Kuijf, B. Tausk, W.T. Giele, *On the Production of a W and Jets at Hadron Colliders*, Nucl. Phys. B357:32-64 (1991).
[9] F. Maltoni, T. Stelzer, *MadEvent: Automatic Event Generation with MadGraph*, JHEP 302, 27 (2003).
[10] M. G. Bowler, Z. Phys. C 11, 32 (1981).
[11] SLD Collaboration, K. Abe et al., Phys. Rev. Lett. **84**, 4300 (2000), arXiv:hep-ex/9912058.
[12] CDF Note 6804, http://hep.uchicago.edu/~hslee/ISR/cdf6804_ISR_DY.ps
[13] D. Wicke and P. Skands, arXiv: 0807.3248v1.
[14] L. Lyons, D. Gibaut and P. Clifford, Nucl. Instrum. Meth. A **270**, (1988) 110;
A. Valassi, Nucl. Instrum. Meth. A **500**, (2003) 391.
[15] The Tevatron Electroweak Working Group for the CDF and $D\bar{O}$ Collaborations *Combination of CDF and $D\bar{O}$ results on the Mass of the Top Quark*, arXiv: 0903.2503 (2009).
[16] $D\bar{O}$ Collaboration, V.M. Abazov et al., Measurement of the top quark mass in nal states with two leptons, to be submitted to PRD.